Surface-plasmon-assisted electron-capture mechanism in low-energy $He^+(1s)$-Al(111) collisions

H. Jouin,[1,*] F. A. Gutierrez,[2] and C. Harel[1]
[1]*CELIA (UMR 5107 du CNRS), Université Bordeaux I, 351 Cours de la Libération, 33405 Talence Cedex, France*
[2]*Departamento de Física, Universidad de Concepción Casilla 4009, Concepción, Chile*
(Received 24 August 2000; revised manuscript received 2 January 2001; published 16 April 2001)

We analyze the neutralization of low-energy $He^+(1s)$ ions interacting with an Al surface under grazing incidence. First, we calculate transition rates for the surface plasmon-assisted mode of ion neutralization. A comparison of these transition rates with Auger rates recently reported in the literature indicates that the collective process is dominant from large to intermediate ion-surface distances. Inclusion of these transition rates into a set of rate equations relevant to the $He^+(1s)$/Al(111) interacting system allows us to compute neutralized fractions and angular distributions of the scattered neutral atoms. Comparison of our results with recent experimental data seems to indicate that proper inclusion of both the Auger and collective surface plasmon rates is essential to explain the experimental results. Finally, a phenomenological rate for transitions into the ground state of He was extracted from experimental angular distributions.

DOI: 10.1103/PhysRevA.63.052901 PACS number(s): 79.20.Rf

I. INTRODUCTION

When a slow ion approaches a metallic surface, several processes can take place due to the potential interaction between the ion and surface. Among these, the ion neutralization process, whereby a metal electron is captured by the incoming ion, has been strongly considered in recent years from both the theoretical and experimental points of view. The interest concerns both fundamental questions as well as technological applications.

The two simplest mechanisms for ion neutralization near metallic surfaces which have been known to exist for a long time are the resonant tunneling mode [1] in which an electron tunnels from a level within the conduction band of the solid to a bound state of the ion-electron system without changing its energy and the direct Auger mode [2] in which two electrons in the conduction band interact in such a way that one of the electrons falls into a lower-energy state of the bound ion-electron system while the second electron absorbs the energy released during the capture going to a state out of the conduction band. At the end of the 1980, a new competing mode, the pure surface-plasmon (PSP) mode, was proposed [3,4] in which one metal electron falls into a low-lying atomic state while a surface plasmon is excited by means of the energy released in the electronic transition. The recent experimental works of Baragiola and Dukes [5] and Niemann *et al.* [6] on ion-induced low-energy electron spectra contain indications of bulk and surface-plasmon excitations during low-energy ion-surface collisions. The collective (multielectron) mode can be viewed as complementary to the (two-electron) Auger mode, as they represents two different regimes of response of the surface to the ion's field.

To analyze theoretically and experimentally the relative importance of the collective mechanism and its contribution to the neutralization process, one has to eliminate the possibility of other processes which can occur if the ion penetrates the solid. For this reason the kinetic energy of the projectile ion must be smaller than the repulsive force produced by its interaction with the surface atoms which is in the eV regime. Unfortunately, it is not a trivial task to produce ion beams with small enough energies. However, at very small angles of incidence (grazing incidence), the energy related to the perpendicular motion of the ion is sufficiently low to prevent the ion from entering significantly into the solid. For instance, for angles of the order of 1°, as in the typical experiments of Winter [7], the energies of the parallel and normal motion differ by about four orders of magnitude so that his keV ion beams have normal energies in the eV domain. As already mentioned in Ref. [7], for this type of experimental arrangement the above-mentioned charge-exchange mechanisms are the most relevants.

The choice of single-charged ions, like H^+ or He^+, as projectiles is clear since multicharged ions can give rise to neutralizations into multiply excited atomic levels which are in resonance with the conduction band with the possibility afterwards of many direct (one-step) or indirect (several-step) transitions besides the one we are interested in. Another crucial and practical consideration in choosing these kind of projectiles is related to the possibility of a realistic theoretical description of the atomic structure of the neutralized ion-electron system in the presence of the surface which is quantitatively unknown in all the cases except for hydrogenlike ions [8,9] and helium atoms [10–12]. Indeed, consideration of the perturbation produced by the surface causes an upward shift of the energy levels and hybridization of the vacuum wave functions, which complicates the evaluations of neutralization rates. On the other hand, the choice of simple metals like Al or Mg is related to the fact that their electronic behavior can be modeled in a good approximation as an electron gas for which several theoretical approaches can be pursued to describe its response to the ion's potential field [13].

*Corresponding author. FAX: (33) 5 57962580. Electronic address: jouin@celia.u-bordeaux.fr

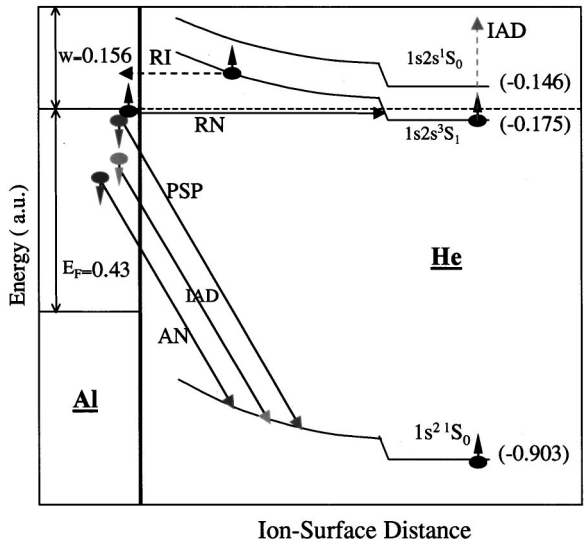

FIG. 1. Energy diagram for He in front of Al and schematic representation of the neutralizing processes involved: AN≡Auger neutralization process, PSP≡pure surface-plasmon process (for simplicity, the ejected Auger electron for the AN process and the surface plasmon for the PSP process are not represented in the figure), IAD≡indirect Auger deexcitation process, RN≡resonant neutralization process, and RI≡resonant ionization process.

Over the last decade several theoretical [14–16] and experimental [7,17] reports have been published in the literature on the problem of ion neutralization for the He^+-Al system under grazing incidence. In Fig. 1 we show a schematic energy diagram of the $He^+(1s)$-Al system to describe the various processes that can lead to the formation of He atoms in very low normal energy collisions. Due to energy conservation, the Auger neutralisation (AN) and PSP processes can only populate the ground state $1s^2(^1S_0)$ of He atoms. This is the only state considered in Refs. [14–16] for the $He^+(1s)$-Al system. However, asymptotically the excited triplet state $1s2s(^3S_1)$ has an energy $(-0.175$ a.u.) which is slightly below the work function $(-0.156$ a.u.). Thus, at large ion-surface separations, this state can be, in principle, populated by means of resonant transitions (RN). Nevertheless, as the atom approaches the surface, the binding energies of atomic levels decreases (see Fig. 1) due to the shift caused by image charge interactions. In fact, for ion-surface distances smaller than 14 a.u., the $1s2s$ triplet level is above the Fermi level so that the resonant capture is energetically forbidden. Therefore, the triplet state can get populated by the resonant mode only for distances larger than 14 a.u. At shorter distances, when the binding energy of the triplet $1s2s$ level becomes smaller than the work function, the few captured electrons can be lost by resonant ionization (RI) towards the unoccupied metal states. These electrons can also be transferred to the ground state via the indirect Auger deexcitation (IAD) process [17]. The direct Auger deexcitation process is forbidden for triplet states because of spin conservation [17,18]. Inclusion of kinematic effects due to parallel motion will shift upwards the Fermi energy [17,19]. In particular, the resonance conditions and the transition rates for the RN and RI processes for populating and depopulating the triplet state will be modified. Indeed, the RN rates have been found to decrease drastically with parallel velocity (see Trubnikov and Yavlinskii [19]). Nevertheless, the global description of the various mechanisms leading to the neutralization of the ions presented above remains correct. Analogous transitions involving higher excited states are energetically forbidden.

The most striking feature of the recent results for the He^+-Al system is the clear disagreement between theory and experiment. The different theoretical reports [14–16] contain an ever-increasing degree of sophistication in the dielectric response of the surface and also in the description of the initial and final states of the captured electron. However, recently Hecht *et al.* [17] have indicated that these theoretical Auger rates, which do not differ very much from each other, are insufficient to explain the experimental angular distribution of 2-keV He^+ ions neutralized at Al surfaces with 0.5° of incidence. The effect of the perturbation of the ion on the initial electron states which increases the Auger rates only at large distances [16] is not enough to produce a change on this situation. We should note that in Refs. [14–16] their Auger rates are supposed to include both the single-particle (electron-hole-pair) response and the collective (surface-plasmon) response of the electron gas to the field of the incoming ion, but in light of the results we obtain in this work, it seems that perhaps they are still missing some important contribution to the neutralization rates for the He^+-Al system.

The main purpose of this work is to analyze the relative importance of the pure surface-plasmon mode of ion neutralization as compared to the Auger mode and to show that proper consideration of both modes can lead to a much better agreement between the theoretical and experimental results. For that purpose we shall calculate transition rates, neutralized fractions, and angular distributions of scattered He atoms in very low perpendicular energy $He^+(1s)$-Al(111) surface reactions in order to compare with the most recent published results.

In Sec. II we develop the theory for collective transition rates, while in Sec. III we indicate all the steps which are necessary to evaluate the neutralized fractions and also the angular distributions. The results and all relevant discussions appear in Sec. IV. The main conclusions are summarized in Sec. V. Atomic units are used throughout this paper unless otherwise stated.

II. THEORY FOR COLLECTIVE TRANSITION RATES

Within the orthogonalized first Born approximation and the fixed ion approximation, the transition rate for the pure surface-plasmon mode of ion neutralization is given by

$$\Gamma_{\mathrm{PSP}}=2\pi\sum_{\mathbf{k},\mathbf{q}<\mathbf{q}_c}|\langle\Phi_n^{(f)},\mathbf{q}|H_{\mathrm{int}}|\Phi_{\mathbf{k}}^{(i)}\rangle|^2\delta(\varepsilon_i-\varepsilon_f), \quad (1)$$

where $\varepsilon_i=\frac{1}{2}k^2$ is the energy of the initial state $|\Phi_{\mathbf{k}}^{(i)}\rangle$, which is orthogonal to $|\Phi_n^{(f)},\mathbf{q}\rangle$ and which represents an electron with momentum $\mathbf{k}$ in the conduction band. The energy $\varepsilon_f(s,q)$ of the final state $|\Phi_n^{(f)},\mathbf{q}\rangle$, for an electron lying on

an atomic state labeled n and for a plasmon of wave vector $\mathbf{q}(q,\varphi_q)$ and energy $\omega_s(q)$, is (with respect to the bottom of the conduction band)

$$\varepsilon_f(s,q)=V_0-E_n(s)+\omega_s(q), \tag{2}$$

with $V_0=E_F+W$ the depth of the conduction band (E_F being the Fermi energy and W the corresponding work function) and $E_n(s)$ the bound energy of the final atomic state which is a function of the ion-image plane distance s due to the atom-surface interaction. The condition $q<q_c$ in Eq. (1) means that Γ_{PSP} contains only the long-range (small-q) surface-plasmon contribution to ion neutralization. It does not include those contributions coming from the regime of short-range (large-q) particle-hole excitations. In general, for low values of the transferred momentum q, it is possible to separate the response of the many electron system to the external Coulomb perturbation, approximately, into a collective surface-plasmon part and an electron-hole excitation part. In fact, for the $q\to 0$ limit, the separation becomes exact, since the electron-hole part of the spectrum disappears and the surface-plasmon peak tends to the δ function. However, for large values of q, it is not possible to separate the two different responses because their contributions overlap in such a way that the concept of well-defined coherent surface-plasmon modes and single-particle excitations breaks down (surface plasmons are strongly damped beyond a certain value of q). In particular, for the He^+-Al system, it has been found [20] that, for distances $s\gtrsim 3$, the important contribution to the neutralizing transition rates comes from the excitation of surface plasmons, whereas for smaller distances, the particle hole channel increases, becoming the most important one inside the metal. Therefore, since for the moment we want to evaluate the pure surface-plasmon channel, we shall consider the range $q<q_c$, with q_c small enough to have well-defined surface-plasmon modes and also ion-surface distances which are not too small. Under these circumstances we can consider the electron-surface plasmon coupling [3,4]

$$H_{\mathrm{int}}=\sqrt{\frac{\pi\omega_s(q)}{q\mathcal{A}}}\,e^{-i\mathbf{q}\cdot\boldsymbol{\rho}}e^{-q|z+s|},\quad q\leqslant q_c, \tag{3}$$

with $\mathcal{A}$ the elementary area, (ρ,φ,z) the electronic cylindrical coordinates (ρ and z being parallel and perpendicular to the surface plane, respectively), and with the origin of electronic coordinates located at the ion's position. Recently, Denton *et al.* [21] have applied this interaction potential to analyze the probabilities of the excitation of surface plasmons when 8-keV electrons are reflected from aluminum surfaces, obtaining a good agreement with an equivalent semiclassical dielectric version of the collective response and also with the experimental results of Powell [22] for the angular dependence of the collective surface excitation. In Ref. [21] (see their Appendix), they include a short review of the quantization of the general electrostatic potential for the interaction of an external charge with a semi-infinite electron gas leading to the expression (3). For the plasmon dispersion relation $\omega_s(q)$ in Al, we have fitted the experimental data of

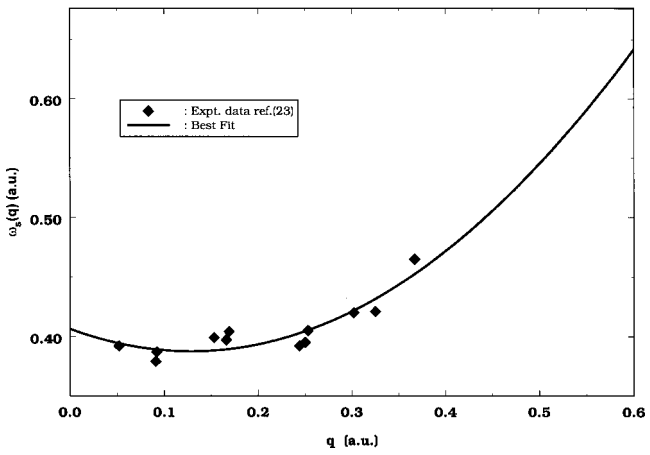

FIG. 2. Surface-plasmon dispersion for Al, i.e., surface-plasmon energy (in a.u.) as a function of the plasmon wave vector modulus q (in a.u.). ◆: experimental data of Tsuei *et al.* [23]. Solid line: best fit of the experimental data (see text).

Tsuei *et al.* [23] by means of the quadratic function $\omega_s(q)=\omega_s^0+\alpha q+\beta q^2$. This is shown in Fig. 2, where we have plotted the experimental data of Ref. [23] as well as our best fit (with parameters $\omega_s^0=0.4064$ a.u., $\alpha=-0.2938$ a.u., and $\beta=1.1430$ a.u.). We should note that there is no experimental data for q larger than 0.37 a.u.; nevertheless, for the calculations of the transition rates, we shall need the dispersion relation up to $q=0.67$ a.u. as a consequence of energy conservation. In those cases, the dispersion relation is extrapolated by means of our fit.

Consideration of the potential ($V_{e\text{-}s}^J$) defined by Jennings *et al.* [24] to describe the electron-surface interaction allows us to write the Hamiltonian for the initial electronic state, embedded in the conduction band of the metal, as

$$H_i^{(J)}=-\frac{1}{2}\nabla^2+V_{e-s}^J, \tag{4}$$

$$V_{e\text{-}s}^J=-\frac{1-e^{-\lambda(z+s)}}{4(z+s)}\Theta(z+s)-\frac{V_0}{(Ae^{B(z+s)}+1)}\Theta(-z-s), \tag{5}$$

with $A=4V_0/\lambda-1$ and $B=2V_0/A$, Θ being the unit step function and $\lambda=1$ a.u. for Al [24]. As stated by Liebsch [13], the distribution of electronic density corresponding to the smooth variation of the potential $V_{e\text{-}s}^J$ in the surface region ($z\simeq -s$) is consistent with the experimentally observed plasmon dispersion relation we are including in the present calculations. In Eq. (4) we do not include the perturbation of the initial metal electron states due to the interaction with the incoming ion. We expect this to be a reasonable approximation due to the weakening of the electron-ion interaction as a consequence of screening. In fact, in recent calculations of collective rates for the H^+-Mg system we have obtained [25], by application of a rather crude approximation, that the ion perturbation has a non-negligible contribution to the rates only in regions (not too close to the surface) where the collective rates themselves are very small compared to the rates

near to the surface. Furthermore, in Ref. [16], they have found that for the $He^+(1s)$/Al system the effect of the perturbation of the initial electron states (due to the presence of the ion) on the Auger neutralization rates becomes noticeable only for ion-surface distances beyond $s\sim 6$, with the corresponding Auger rates being more than three orders of magnitude smaller than the rates around $s\sim 2$. Therefore, in order to avoid introducing unnecessary complications into the present calculations, we shall disregard in what follows this effect, although we shall partially consider the effect of the ion on the initial electron state by orthogonalizing it with respect to the final bound electron state.

The z part of the wave function $F_{k_z}(z)$ corresponding to the Hamiltonian of Eq. (4) is calculated numerically by means of the Numerov algorithm. Then the initial electronic wave function reads

$$|\Phi_{\mathbf{k}}^{(i)}\rangle = e^{i\mathbf{k}_\rho\cdot\boldsymbol{\rho}} F_{k_z}(z), \tag{6}$$

where $\mathbf{k}_\rho(k_\rho,\varphi_k)$ and k_z are the components of the initial electronic momentum parallel and perpendicular to the surface plane, respectively.

Among all the possible final bound electron states, we are only interested in the ground state of He, since, the collective surface-plasmon channel cannot populate the excited levels. Indeed, for these states, the energy released during electron capture is not enough to excite a surface plasmon. Therefore, for the He atom in front of an Al surface, we consider the Hamiltonian

$$H_f = -\frac{1}{2}\nabla^2 + V_{e\text{-}s}^J + V_{e\text{-}i} + \Delta V, \tag{7}$$

with $V_{e\text{-}s}^J$ the electron-surface interaction of Jennings *et al.* [24], already given in Eq. (5), and where $V_{e\text{-}i}$ represents the intra-atomic electron-core interaction which has been described elsewhere [12] through the Bottcher (singlet) potential [26] since it reproduces pretty well the observed energy levels of the isolated (vacuum) He atom. We shall also consider the Bottcher potential ($V_{e\text{-}i}^B$) here. The last term in Eq. (7) is the usual electron-ion (image) potential, which takes into account the change in the electron-surface interaction due to the presence of the positive ion. Explicit expressions for $V_{e\text{-}i}^B$ and for ΔV are, respectively

$$V_{e\text{-}i}^B(r) = -\frac{1}{r} - \left(4+\frac{1}{r}\right)e^{-4r} - \sum_{j=1}^{4} c_j r^{j-1} e^{-2r}, \tag{8}$$

with $r=\sqrt{\rho^2+z^2}$ ($c_1=-8.9595$, $c_2=29.4240$, $c_3=-20.8924$, $c_4=3.6381$) and

$$\Delta V(\rho,z) = \frac{\theta(z+s)}{\sqrt{\rho^2+(z+2s)^2}}. \tag{9}$$

As described in previous works [12,27], the eigenfunctions $|\Phi_n^{(f)}\rangle$ of H_f are calculated by means of a diagonalization method using a basis set of hydrogenic parabolic orbitals $u_{n_1,n_2,m}(\rho,\varphi,z)$ [28] [for these orbitals, the principal quantum number n^* is related to the parabolic quantum numbers (n_1,n_2,m) by $n^*=n_1+n_2+m+1$]. In this way, one obtains the eigenfunctions as linear combinations of the basis orbitals,

$$|\Phi_n^{(f)}\rangle = \sum_{i=1}^{N} C_{ni}(s)|u_i\rangle, \tag{10}$$

and the corresponding eigenenergies $E_n(s)$ which depend on the ion-image plane distance s due to the interaction between the final atomic state and the various image charges. In Eq. (10), the size of the basis set (N) is increased until the eigenvalues are independent (within the desired accuracy) of the number of basis orbitals. To represent the ground state of He in front of the Al surface, we have checked that it is sufficient to include in expansion (10) $N=6$ hydrogenic parabolic orbitals (i.e., all the $m=0$ orbitals up to the $n^*=3$ shell). The main result for this system is that the energy shifts follow an image charge behavior $1/4s$ even up to distances $s=2$. At this distance the energy shift of the ground state of He is 3.5 eV, which is comparable to the work function of Al. More details are given in Ref. [12].

After an analysis analogous to the one performed in [4], the transition rate of Eq. (1) becomes

$$\Gamma_{\mathrm{PSP}}^n(s) = \frac{1}{8\pi^3}\int_{q_{\min}}^{q_{\max}} dq\ \omega_s(q) \int_0^{\sqrt{2\varepsilon_f(s,q)}} dk_z \int_0^{2\pi} d\varphi_k \times \int_0^{2\pi} d\varphi_q |\mathcal{M}_{\mathbf{k}}^{n,\mathbf{q}}(k_z,\varphi_k;q,\varphi_q)|^2, \tag{11}$$

where the matrix element $\mathcal{M}_{\mathbf{k}}^{n,\mathbf{q}}$ is

$$\mathcal{M}_{\mathbf{k}}^{n,\mathbf{q}} = \sum_{j=1}^{N} C_{nj}(s)\mathbb{M}_j^{(1)}(k_z,\varphi_k;q,\varphi_q) - \sum_{m=1}^{\mathcal{P}} \left\{ \left[\sum_{i=1}^{N} C_{mi}(s)\mathbb{O}_i(k_z,\varphi_k) \right] \times \left[\sum_{j=1}^{N}\sum_{i=1}^{N} C_{mi}(s)C_{nj}(s)\mathbb{M}_{ij}^{(2)}(q) \right] \right\}. \tag{12}$$

The matrix elements $\mathbb{M}_j^{(1)} = \langle u_j | e^{-q|z+s|} e^{-i\mathbf{q}\cdot\boldsymbol{\rho}} | \Phi_{\mathbf{k}}^{(i)}\rangle$, $\mathbb{O}_i = \langle u_i | \Phi_{\mathbf{k}}^{(i)}\rangle$ and $\mathbb{M}_{ij}^{(2)} = \langle u_i | e^{-q|z+s|} e^{-i\mathbf{q}\cdot\boldsymbol{\rho}} | u_j\rangle$ are calculated numerically by means of Gauss-Laguerre and Gauss-Legendre quadratures. In Eq. (12), $\mathcal{P}$ corresponds to the number of final atomic eigenfunctions included in the orthogonalization procedure (see [27]). In the present calculation, the initial state $|\Phi_{\mathbf{k}}^{(i)}\rangle$ is orthogonalized to the perturbed ground state of He, i.e., to the final bound electron state $|\Phi_n^{(f)}\rangle$. It is important to note at this point that the conservation of the energy in conjunction with the energy shifts of the atomic level and the constraint $k\leqslant k_F$ (k_F being the Fermi wave vector modulus) for the metal electron wave vector leads, as a consequence, to the appearance of a threshold ion-surface distance s_0 below which the plasmonic rates vanish independent of the values of q. In particular, for the $He^+(1s)$-Al system we obtain $s_0\simeq 1$ a.u. when plasmon dis-

persion is taken into account. On the other hand, for each ion-surface distance, the same constraints fix the limits of integration over q appearing in Eq. (11) through the inequality

$$0<\varepsilon_f(s,q)\leqslant E_F. \tag{13}$$

As an example for the He^+-Al system investigated here and for $s=3$, Eq. (13) leads to $q_{\max}=0.61$ a.u., whereas for $s=10$, one has $q_{\max}=0.66$ a.u. In all cases, $q_{\min}=0$.

III. THEORY FOR NEUTRALIZED FRACTIONS AND ANGULAR DISTRIBUTIONS

In order to compute the occupations corresponding to the ground state of the ion (P^+), to the ground state of the neutral atom (P^g), and to the triplet ($1s2s\ ^3S_1$) state (P^t), we solve (by means of a Runge-Kutta method) the following set of coupled rates equations:

$$\begin{aligned} \boxed{dP^+/dt=-(\Gamma_{\rm AN}+\Gamma_{\rm PSP})P^+} &-g_t\Gamma_{\rm RN}P^+ +\Gamma_{\rm RI}P^t,\\ \boxed{dP^g/dt=+(\Gamma_{\rm AN}+\Gamma_{\rm PSP})P^+} &+\Gamma_{\rm IAD}P^t,\\ dP^t/dt=+g_t\Gamma_{\rm RN}P^+ &-\Gamma_{\rm RI}P^t-\Gamma_{\rm IAD}P^t, \end{aligned} \tag{14}$$

with the initial conditions $P^+(t\to-\infty)=1$ and $P^g(t\to-\infty)=P^t(t\to-\infty)=0$ and the normalization $P^+(t)+P^g(t)+P^t(t)=1(\forall\, t)$. Here g_t is the spin statistical factor for capture into the triplet state ($g_t=3/2$). In the case where the triplet state population is not taken into account, this set reduces to the simple form within boxes in the above equations. The PSP rates ($\Gamma_{\rm PSP}$) are those obtained as indicated in Sec. II. For the Auger neutralization rates, we have used the one computed by Lorente *et al.* [16] (we have also performed calculations with those previously calculated by Lorente and Monreal [15]). The resonant transition rates ($\Gamma_{\rm RN},\Gamma_{\rm RI}$) are those calculated by Makhmetov *et al.* [11] by means of a nonperturbative approach. For the indirect Auger deexcitation transition rates ($\Gamma_{\rm IAD}$), actually there is a lack of *ab initio* calculations, so that for this process, we have used the transition rates computed by Hecht *et al.* [17] in a procedure that starts from the experimental angular distribution of scattered neutrals atoms in the $He^+(1s)$-Al(111) collision.

As all these transition rates are calculated as a function of the ion-image plane distance s, in order to integrate the set of coupled rates equations, we use the transformation

TABLE I. Parameters of the ZBL screening potential.

i	1	2	3	4
α_i	0.0282	0.2802	0.5099	0.1818
β_i	0.2016	0.4029	0.9423	3.1998

$$dt=\frac{ds}{v_\perp(s)}, \tag{15}$$

where $v_\perp(s)$ is the perpendicular velocity of the ion. This velocity is computed by means of energy conservation for the ion motion:

$$v_\perp(s)=\sqrt{\frac{2}{M_I}}\sqrt{E_{\perp 0}-U_T(s)}, \tag{16}$$

with M_I the ion mass, $E_{\perp 0}$ its total energy corresponding to the normal motion, and $U_T(s)$ the total scattering potential experienced by the ion. This total scattering potential is the sum of a repulsive potential $U_R(s)$ due to the first atomic plane and an attractive potential $U_A(s)$ produced by the interaction of the ion with its own image charge:

$$U_T(s)=U_R(s)+U_A(s). \tag{17}$$

The repulsive term is obtained as described in Gemmel's review [29] by averaging over the first atomic plane individual interatomic potentials. In this work, the interatomic potential is represented by a Ziegler-Biersack-Littmark (ZBL) screening potential [30]. This leads to the following expression for the ideal planar repulsive potential:

$$U_R(s)=2\pi\mu Z_I Z_S a\sum_{i=1}^{4}\left(\frac{\alpha_i}{\beta_i}\right)\exp\left[-\left(\frac{\beta_i}{a}\right)(s+d_{\rm im})\right], \tag{18}$$

where μ is the density of surface atoms per unit of area [$\mu=0.0394$ for Al(111)], Z_I and Z_S are the atomic numbers of the ion and surface atoms, respectively ($Z_I=2$ and $Z_S=13$ in this particular case), and a is the screening length [$a=0.8854(Z_I^{0.23}+Z_S^{0.23})^{-1}$]. The parameters α_i and β_i are listed in Table I. For the distance between the first atomic plane and the image plane $d_{\rm im}$, we have used the result computed by Serena *et al.* [31] for Al(111): $d_{\rm im}=3.295$ a.u.

For the attractive image potential $U_A(s)$, we have used the form based on the Thomas-Fermi approximation proposed by Kato *et al.* [32]:

$$U_A(s)=\begin{cases} -Q^2\dfrac{1}{4s}\displaystyle\int_0^\infty du\,\exp(-u)\left[\frac{u}{2k_{\rm TF}s}-\left(\frac{u^2}{(2k_{\rm TF}s)^2}+1\right)^{0.5}\right]^2 & \text{for } s>0,\\ -Q^2\dfrac{k_{\rm TF}}{3} & \text{for } s=0,\\ -Q^2\dfrac{k_{\rm TF}}{4}\left[2+\dfrac{\exp(-2k_{\rm TF}|s|)}{k_{\rm TF}|s|}-4\displaystyle\int_0^\infty du\,\frac{u\exp(-2k_{\rm TF}|s|\sqrt{u^2+1})}{u+\sqrt{u^2+1}}\right] & \text{for } s<0, \end{cases} \tag{19}$$

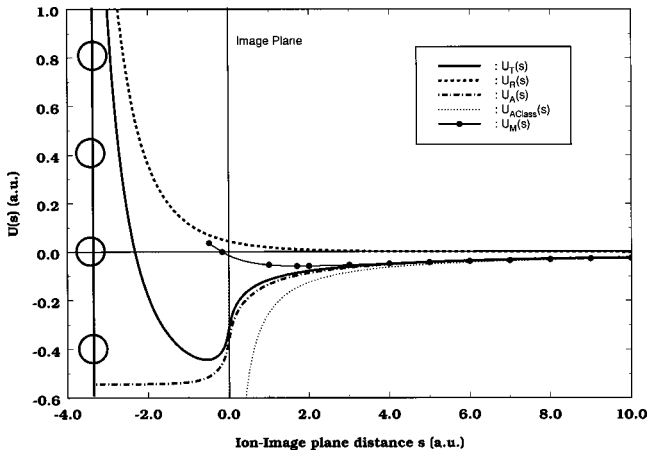

FIG. 3. Scattering potentials as a function of the ion-image plane distance *s*. Solid line: total potential experienced by the ion during its approach ($U_T = U_R + U_A$). Dashed line: planar repulsive potential (U_R). Dot-dashed line: attractive image potential defined by Kato *et al.* [32] (U_A). Dotted line: classical image potential, i.e., asymptotic part of the image potential of Kato *et al.* ($U_{A\infty} = -1/4s$). Solid line with circles: total scattering potential calculated by Merino *et al.* [35]. The vertical line with open circles located at $s = -3.295$ a.u. represents the first atomic plane, while the vertical line located at $s = 0$ represents the image plane.

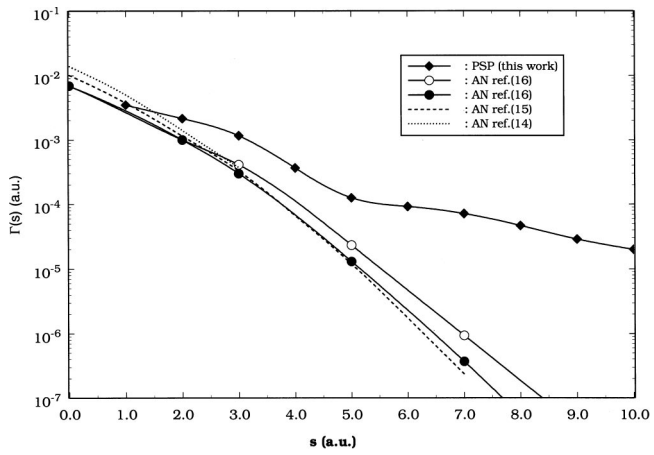

FIG. 4. PSP and AN transition rates for the $He^+(1s)$-Al system (in a.u.) as a function of the ion-image plane distance (in a.u.). ♦: PSP transition rate calculated in this work. ○ and ●: AN transition rates calculated by Lorente *et al.* [16] (○,●: with and without inclusion of the ion effect on the initial electronic wave function, respectively). Dashed line: AN transition rate computed by Lorente and Monreal [15] (interacting case). Dotted line: AN transition rate of Alducin *et al.* [14].

with Q the ion charge ($Q = 1$ in this work) and k_{TF} the Thomas-Fermi wave number: $k_{TF} = 1.5632/\sqrt{r_s}$, where $n_e = (\frac{4}{3}\pi r_s^3)^{-1}$ is the electronic density of the solid ($r_s = 2.07$ in case of Al). In Fig. 3, we have plotted, for $He^+(1s)$-Al(111), the total scattering potential as a function of the ion-image plane distance, as well as the repulsive and attractive parts and also the asymptotic form of the attractive image potential ($U_{A\infty} = -1/4s$), i.e., the classical image charge potential.

In order to obtain the angular distribution of scattered neutral atoms in the ground state, we calculate for each integration interval ds of coupled rates equations [Eq. (14)], the elementary fraction of ions which are neutralized in the ground state (i.e., dP^g). For very low perpendicular velocities like those considered here, there is no re-ionization mechanism in close encounter collisions. Moreover, in the collision investigated in this work, the parallel velocity is too low ($v_\parallel = 0.14$ a.u.) to allow the loss mechanism proposed by Winter [7]. Therefore, once the ground state is populated, the He atoms can not experiment further transitions, remaining as neutral He($1s^2$) atoms. At the instant of neutralization, the attractive image potential vanishes and then the neutral atoms in the ground state are reflected by the planar potential in a direction given by the composition of the parallel velocity ($v_\parallel$, which is a constant here because corrugation effects are not considered) and the perpendicular velocity aquired by the ion at the distance corresponding to its neutralization $v_\perp(s^\star)$. Then the corresponding outgoing angle φ is given by

$$\tan\varphi = \frac{v_\perp(s^\star)}{v_\parallel}. \tag{20}$$

Angular distributions are obtained by arranging the elementary neutral fractions dP^g according to their outgoing angle. The convergence of this approach might be checked by decreasing the integration step ds (typically, here, $ds \approx 5 \times 10^{-3}$ a.u. to obtain accurate results). Afterwards, the theoretical angular distribution is convoluted by means of a gaussian shape of width $\delta\varphi = 0.08°$ in order to account for the experimental angular resolution [17]. Finally, the angular distributions presented below are normalized in such a way that their area correspond to the fraction of scattered atoms in the ground state [i.e., $P^g(t \to +\infty)$]. The experimental angular distribution [17] was normalized in the same way.

IV. RESULTS AND DISCUSSION

A. Transition rates

In Fig. 4 we show our PSP rates Γ_{PSP}, given as a function of the ion-image plane distance, for the neutralization of He^+ at Al surfaces. For purposes of comparison we also include there the most recent Auger rates of Lorente *et al.* [16] for both unperturbed and perturbed (due to the ion) metal electron states, those of Lorente and Monreal [15] for what they call the interacting case, and those of Alducin *et al.* [14]. Note that all the Auger rates which do not contain the effect of the ion on the metal electron states remain very close to each other except in the region $s < 2$ where they differ by a factor smaller than 2. Clearly, the PSP curve goes well above both the perturbed and unperturbed Auger curves for distances $s \geqslant 3$, although for shorter distances the curves become closer in such a way that near $s = 1.5$ the Auger rate of Alducin *et al.* [14] takes over with the PSP rate vanishing below $s = 1$ as a consequence of the constraint imposed by the conservation of the energy together with the upward shift of the bound energy levels and the condition $k < k_F$. All the other Auger rates remain below Γ_{PSP} for $s > 1$. On the other

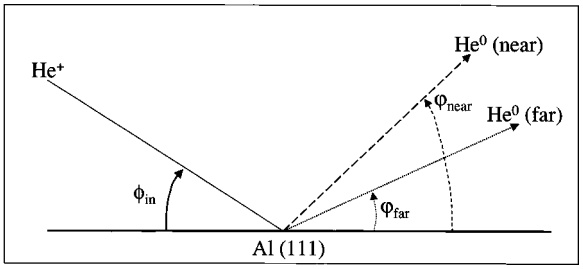

FIG. 5. Schematic representation of the image potential effects on the outgoing angles φ of neutralized particles depending on the location of the neutralization: small outgoing angles for particles neutralized far from the surface and large outgoing angles when the neutralization occurs close to the surface.

hand, the effect of the perturbation of the metal electron states by the ion included in the AN rates of Ref. [16] starts to be noticeable at distances where the Auger curve itself has already decayed several orders of magnitude so that one would expect that its contribution to the angular distribution and neutralization fraction is relatively small. The variation of the slope of the PSP transition rate around $s=5$ can be unambiguously related to the contribution of the $n^*=2$ shell to the expansion of Eq. (10) for the final bound-electron state, which at this distance starts to be comparable to the most important contribution coming from the $n^*=1$ shell. We shall come back to this point later.

As already mentioned in the Introduction, in Refs. [15, 16] the authors indicate that their Auger rates include both the single-particle response and the collective response of the electron gas to the field of the incoming ion. If one accepts the correctness of the PSP rate, then Fig. 4 indicates that they might be losing some important contributions to the total neutralization rate. In fact, recently Hecht *et al.* [17] have indicated that these theoretical Auger rates are insufficient to explain the angular distribution of 2-keV He^+ ions neutralized at Al surfaces with 0.5° of incidence. In the next subsection, we shall show that consideration of our collective PSP rates into a set of rate equations leads to angular distributions not too far from the experimental ones. That is not the case for the Auger rates. However, the proper consideration of both the PSP rates and the Auger rates makes the agreement with the experiment even better.

B. Angular distributions

It is now well known that the attractive image forces have an important effect on the trajectories of the ions in grazing incidence collisions [33]. On the other hand, as shown in the previous section, the Auger transition rates strongly decrease as a function of the ion-surface distance, the PSP process being dominant at large ion-surface separations. So the ions which are neutralized through the PSP mechanism (far from the surface) are weakly accelerated by the image forces and, hence, emerge with smaller scattering angles than those neutralized close to the surface which are strongly accelerated via the image potential $U_A(s)$: a schematic representation of these features is presented in Fig. 5. Hence a comparison of calculated charge fractions and angular distributions of scattered atoms with experimental results obtained for very low perpendicular impact energy might allow one to obtain informations on the relevancy of the various processes presented above. In what follows, we will essentially use the charge fraction and the angular distribution obtained by Hecht *et al.* [17] for 2-keV $He^+(1s)$ ions impinging on an Al(111) surface with an angle of incidence $\phi_{in}=0.5°$ under ''random'' azimuthal orientation with respect to the directions in the (111) plane. It must be noted that the dynamical calculations presented below also correspond to a ''random'' azimuthal orientation due to the fact that the scattering potential used in this work does not take explicitly into account the crystallographic structure of the (111) plane [the crystallographic structure only appears in our calculations through the parameter μ of Eq. (18)].

It is interesting to note that a simple analysis of the total scattering potential allows one to obtain valuable information about the range of outgoing angles φ available for the scattered neutral particles. Indeed, consideration of the total scattering potential minimal value U^{min} (which corresponds to the highest velocity of the incoming ion) together with Eqs. (16) and (20) allows one to obtain the maximal outgoing angle φ_{max}. Moreover, in the limit of zero image force, which occurs when the ion is neutralized very far from the surface, one expects the usual specular reflection so that $\varphi_{min}=\phi_{in}$. It is clear that corrugation effects will broaden a little bit the angular distributions of scattered particles in such a way that for a clean surface and sufficiently high parallel velocities, φ_{max} can be slightly higher than the value calculated by means of U^{min} and φ_{min} can be slightly smaller than ϕ_{in}. Consideration of the collisional parameters ($E_{in}=2$ keV, $\phi_{in}=0.5°$) corresponding to the $He^+(1s)$-Al(111) collision investigated by Hecht *et al.* [17] and of the minimal value of the total scattering potential in the region ($s\geqslant 0$) where the transition rates are defined [i.e., $U^{min}=U_T(s=0)\simeq -0.3$ a.u.] leads to the following range of outgoing angles: $0.5°\lesssim\varphi\lesssim 3.7°$. These values are consistent with the range of outgoing angles measured by Hecht *et al.* [17]: $1.0°\lesssim\varphi_{expt}\lesssim 3.0°$ with the maximum of the angular distribution around 1.95°. The difference between the lower angles is due to the fact that neutralization starts to be effective at finite ion-image plane separations (around $s\approx 13$ a.u. in the present case). In a recent work dealing with potential electron emission in the $He^+(1s)$-Al(111) reaction at grazing incidence, van Someren *et al.* [34] have used for the He^+-Al system a potential calculated by Merino *et al.* [35] which has been plotted in Fig. 3 [$U_M(s)$: solid line with circles]. As can be noticed in this figure, near the image plane, this potential strongly differs from the one used in the present work: its minimal value $U_M^{min}\simeq -0.058$ a.u. is located around $s\simeq 1.7$ a.u., whereas in our case the minimal value $U_T^{min}\simeq -0.44$ a.u. is located around $s\simeq -0.7$ a.u. (one must recall that as the transition rates are defined only for $s\geqslant 0$, the $s<0$ parts of the scattering potentials do not contribute to the calculations of angular distributions). When the value U_M^{min} is used together with the collisional parameters corresponding to the experiment of Hecht *et al.* [17], one obtains a range of outgoing angles that is much more re-

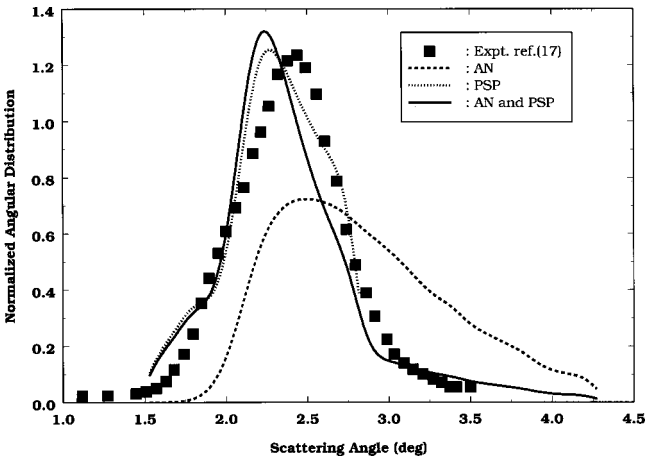

FIG. 6. Normalized angular distributions of neutral He atoms as a function of the scattering angle ($\phi_{in}+\varphi$). Calculations without inclusion of the triplet-state population mechanism (see text): Dashed line: only the AN process is included (transition rates of Lorente *et al.* [16]). Dotted line: only the PSP process is included (transition rates calculated in this work). Solid line: both the AN and PSP processes are taken into account. ■: experimental result of Hecht *et al.* [17].

duced than the previous one, $0.5° \lesssim \varphi \lesssim 1.7°$, and which clearly disagrees with the measurements of Hecht *et al.* [17]: in particular, the maximum of the measured distribution is located out of this range. In other words, the potential used by van Someren *et al.* [34] is not attractive enough in order to reproduce the angular distribution measured by Hecht *et al.* [17]. In fact, the maximal outgoing angle of 3° observed in the experiment corresponds to a value of -0.2 a.u. for the scattering potential, which is very far from the minimal value of the potential used by van Someren *et al.*

In Fig. 6, we present a comparison between the experimental angular distribution of Ref. [17] and our computed angular distributions. For all the calculated angular distributions presented in Fig. 6, the mechanism proposed by Hecht *et al.* [17] leading to a transient population of the triplet state $1s2s\ ^3S_1$ has not been considered. When one takes into account only the Auger process (transition rates of Lorente *et al.* [16]), one obtains the angular distribution represented by the dashed line in Fig. 6. This angular distribution has a maximum around 2.5° and presents an important contribution at large scattering angles which does not appear in the experimental result. This contribution indicates that in their case a great part of the neutralization takes place at too small ion-surface separations. Moreover, the neutral fraction obtained in this case is 90.8%, while in the experiment, a complete neutralization is observed. In their work, Lorente *et al.* [16] indicate that the introduction of their AN transition rate in a set of semiclassical rates equations allows one to obtain the complete neutralization for a 2-keV incident beam at 0.5° from the surface (i.e., the same collision as the one investigated here). In our opinion, the disagreement between both calculations comes from the fact that the acceleration of the ion by the image forces has not been included in the calculation of Lorente *et al.* [16]: indeed, we have checked that neglecting the image effects in our procedure, we obtain a complete neutralization of the beam. This result shows the importance of the image acceleration in such grazing incidence collisions.

We have also performed calculations by using the Auger transition rates calculated by Lorente and Monreal [15] (results not shown in the figure): the shape of the angular distribution obtained in this case is very similar to the one obtained with the AN rate of Lorente *et al.* [16]. This result is not very surprising because one can notice in Fig. 4 that both Auger transition rates are very close except at large distances. From this, we conclude that the perturbation of the initial electron state by the incoming ion does not contribute importantly to the angular distributions.

The dotted line in Fig. 6 represents the angular distribution obtained when the PSP process alone is included, the corresponding neutralized fraction being 92.5%. As can be observed, there is a good overall agreement with the experimental result. However, for scattering angles greater than 2.8°, the computed angular distribution fails to reproduce the experimental data. This is related to the fact (shown in Fig. 4) that the PSP rate vanishes for ion-surface distances smaller than $s_0=1$ due to energy conservation for the PSP process. Nevertheless, if parallel velocity effects were taken into account, we would expect that the PSP rate would become finite up to $s=0$. One can also observe that the calculated angular distribution, which has its maximum around 2.25°, is slightly shifted towards small scattering angles with respect to the experimental one, the maximum of which is observed around 2.4°. This shift indicates that the PSP transition rate computed in this work is overestimated at large ion-surface separations. As already pointed out, the particles neutralized at large ion-surface distances (essentially by the PSP process) are scattered at small angles due to the image effects. We believe that the overestimation of the PSP rate, caused by the strong contribution of the $n^*=2$ shell at large distances, is related to the approximate description of the final He atom as a bound He^+-electron system whose intraatomic interaction is described here with the help of the Bottcher model potential. In fact, we expect that the proper description of the perturbed He atom near the metal surface, which should include the strong interaction between the two bound electrons, should lead to theoretical angular distributions for the PSP mode of neutralization whose behavior should be closer to the experimental one.

When both the Auger and pure plasmon processes are taken into account, the neutral fraction reaches the value of 99.3%, while the corresponding angular distribution (solid line in Fig. 6) partially loses agreement with the experimental result. This distribution is slightly more shifted towards small angles (maximum around 2.2°) than the one related to the PSP mode alone due to the small additional contribution of the AN process at large distances. However, within the fixed ion approximation, the contribution of AN rates at small distances ($0 \leqslant s \leqslant 1$) allows one to reproduce fairly well the fall of the experimental data at large scattering angles.

We could summarize the previous discussion in an equivalent way by consideration of the freezing distance s_f which is defined [16] as the distance where the variation of

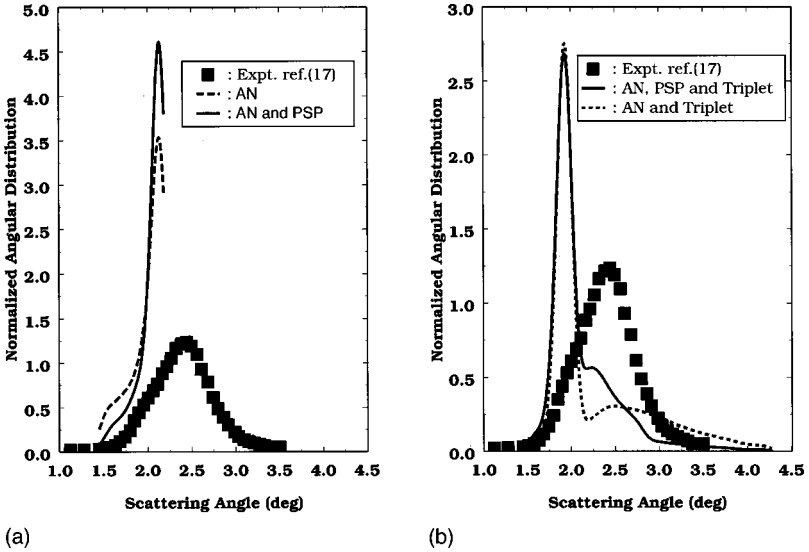

FIG. 7. Normalized angular distributions of neutral He atoms as a function of the scattering angle ($\phi_{in}+\varphi$). (a) Calculations using the potential of Merino *et al.* [35] (see text): Dashed line: only the AN process is included (transition rates of Lorente *et al.* [16]). Solid line: both the AN and PSP processes are taken into account. ■: experimental result of Hecht *et al.* [17]. (b) Calculations including the triplet-state population mechanism (see text): Dashed line: the AN process is also included (transition rates of Lorente *et al.* [16]). Solid line: both the AN and PSP processes are taken into account in addition to the triplet mechanism. ■: experimental result of Hecht *et al.* [17].

the ion population with s is maximum [i.e., $dP^+(s)/ds$ is maximum for $s=s_f$]. For the PSP rate (with and without inclusion of the AN rates), we obtain a freezing distance $s_f \simeq 2.7$ a.u., which is very close to the experimental estimate of 3 a.u. given by Hecht *et al.* [17]. On the other hand, the AN rate of Lorente *et al.* [16] alone yields $s_f=0.7$ a.u. We note that these two freezing distances were obtained considering the image forces which accelerate the ion. If one considers constant velocity for the rate of Lorente *et al.*, then the value $s_f=1.7$ a.u. is obtained, which is very close to the value (1.5 a.u.) reported in their papers [16].

In Fig. 7(a), we present a comparison between the experimental result and calculations in which the total scattering potential computed by Merino *et al.* [35] (and used by van Someren *et al.* [34] in their simulations of electron spectra) has been used instead of the one presented in this work. The transition rates are the same as previously (those calculated by Lorente *et al.* [16] for Γ_{AN} and those obtained in the present work for Γ_{PSP}). From Fig. 7(a), it is clear that with or without inclusion of the PSP rates, the calculated angular distributions strongly differ from the experimental one in both position and intensity. Moreover, in agreement with our previous analysis concerning the range of outgoing angles associated with the potential of Merino *et al.* [35] in the case of the collision studied by Hecht *et al.* [17], the computed angular distributions vanish for scattering angles greater than 2.2° (outgoing angles greater than 1.7°).

In Fig. 7(b), we present a comparison between the experimental angular distribution and calculated angular distributions in which the population mechanism of the triplet $1s2s\ ^3S_1$ state proposed by Hecht *et al.* [17] has been included. For the resonant transition rates (Γ_{RN},Γ_{RI}) needed to integrate the set of coupled rates equations (14), we have used the results obtained by Makhmetov *et al.* [11] by means of the coupled angular modes (CAM) method. For the indirect Auger deexcitation process (Γ_{IAD}), the transition rates computed by Hecht *et al.* [17] have been used. As previously, the Auger neutralization transition rates are those of Lorente *et al.* [16]. One can notice in Fig. 7(b) that with (solid line) or without (dashed line) the PSP process, the calculations disagree with the experimental result. In both cases, the calculated angular distribution presents a very sharp peak around 1.9°, while the experimental one is wider and presents a maximum at 2.45°. The disagreement essentially comes from the fact that the indirect Auger deexcitation transition rate deduced by Hecht *et al.* [17] is strongly overestimated. This overestimation makes the triplet state populated by the resonant process at large ion-surface separations decay rapidly to the ground state (also at large distances), producing a great amount of neutral particles scattered at small angles, as can be observed in Fig. 7(b). One can note that the result obtained by Hecht *et al.* [17] concerning the Γ_{IAD} transition rate is in contradiction with earlier reports found in the literature: on the one hand, Goldberg *et al.* [36] indicate that they have found this transition rate to be negligible; on the other hand, Alducin [18] in *ab initio* calculations has obtained a negligible transition rate for the IAD process from the singlet $1s2s\ ^1S_0$ state. Moreover, we shall see in the next subsection that it is not necessary to introduce the triplet-state population mechanism in order to reproduce the experimental result.

C. Phenomenological transition rates

In their work, Hecht *et al.* [17] extract AN transition rates (Γ_{AN}) and indirect Auger deexcitation transition rates (Γ_{IAD}) starting from the experimental angular distribution of scattered neutral atoms obtained for 2 keV and 0.5° of incidence. They introduce Γ_{AN} and Γ_{IAD} by means of single-exponential decays $\Gamma_i=A_i\exp(-\alpha_i s)$ ($i\equiv$AN,IAD) with ion-surface distance where A_i and α_i are adjustable parameters. In their procedure they iterate over the four parameters in order to reproduce in the best possible way the experimental angular distribution. They need to introduce the triplet state population mechanism (and by the way the IAD transition rate) in order to reproduce accurately the experimental result in particular at small scattering angles. The need to introduce this mechanism is probably related to the use of the classical image charge potential [i.e., $U_{A\infty}(s)=-1/4s$, dotted line in Fig. 3]. As can be observed in Fig. 3, the classical image potential decreases much more rapidly than

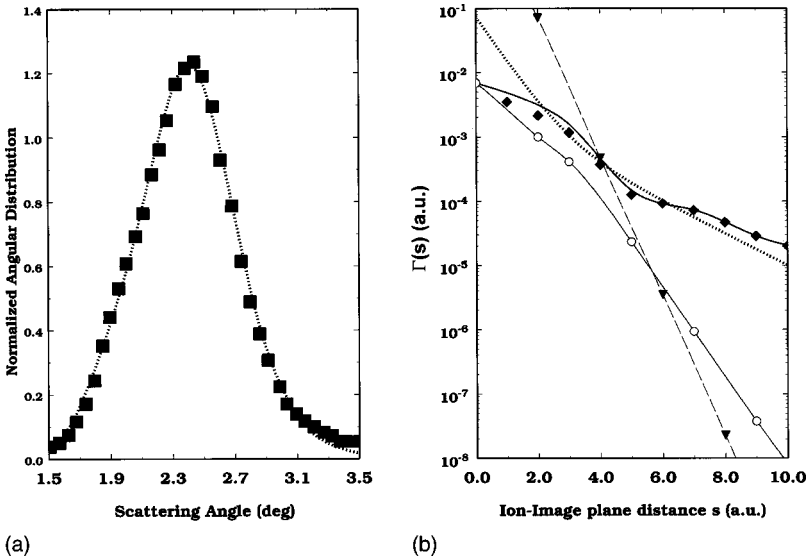

FIG. 8. Results of the fitting procedure (see text). (a) Normalized angular distributions as a function of the scattering angle ($\phi_{in}+\varphi$): ■: experimental result of Hecht *et al.* [17]. Dotted line: angular distribution resulting from the fitting procedure. (b) Transition rates as a function of the ion-image plane distance *s*: Dotted line: transition rate resulting from the fitting procedure (Γ_T). ○: AN transition rate of Lorente *et al.* [16] (Γ^L_{AN}). ◆: PSP transition rate calculated in this work (Γ_{PSP}). Solid line: sum of both previous transition rates ($\Gamma^L_{AN}+\Gamma_{PSP}$). ▼: transition rate deduced by Hecht *et al.* [17].

the potential of Kato *et al.* [32] used in the present work (dot-dashed line in Fig. 3) for intermediate to small ion-image plane distances. So, when the classical image charge potential is considered, the neutral atoms emerge at greater scattering angles than in the case of the potential of Kato *et al.* Therefore, the angular distributions are very sensitive with respect to the representation of the image potential, in particular in the crucial region close to the surface.

We have implemented here a procedure similar to the one proposed by Hecht *et al.* [17], but instead of introducing the triplet-state population mechanism, we have introduced the total rate Γ_T, which contains all the contributions to the neutralization into the ground state, to solve the rate equations

$$dP^+/dt=-\Gamma_T P^+,$$
$$dP^g/dt=+\Gamma_T P^+, \tag{21}$$

where Γ_T is expressed by means of the sum of the two exponential decays:

$$\Gamma_T=A\exp(-\alpha s)+B\exp(-\beta s). \tag{22}$$

In Fig. 8(a), we present the angular distribution obtained by this fitting procedure (dotted line) as well as the experimental one (squares). In Fig. 8(b), we report the corresponding transition rate Γ_T (the best-fit parameters are $A=3.0\times10^{-3}$, $\alpha=0.57$; $B=70.4\times10^{-3}$, $\beta=1.64$). We have also plotted in this figure the AN transition rate of Lorente *et al.* (Γ^L_{AN}) [16] (circles), the PSP transition rate (Γ_{PSP}) calculated in this work (diamonds), the sum ($\Gamma^L_{AN}+\Gamma_{PSP}$) of both previous transition rates (solid line), and the AN transition rate obtained by Hecht *et al.* [17] in their fitting calculation (triangles). This last transition rate strongly disagrees with both the AN transition rate calculated *ab initio* by Lorente *et al.* [16] and also with the result of the present fitting approach.

For distances greater than 6 a.u., Γ_{PSP} and the sum $\Gamma^L_{AN}+\Gamma_{PSP}$ are slightly above the result of the present fitting procedure Γ_T (there is a factor of 2 between Γ_{PSP} and Γ_T at $s=10$): this confirms the overestimation of the PSP process transition rates at large distances. However, as is clear from Fig. 6 (see Sec. IV B), the effect of the overestimation of the PSP rate at large distances does not affect drastically the close behavior of the theoretical angular distribution for the PSP mode of neutralization with respect to the experimental results. For ion-surface distances between 2 and 6 a.u., the sum $\Gamma^L_{AN}+\Gamma_{PSP}$ is very close to Γ_T, while for *s* lower than 2 a.u., $\Gamma^L_{AN}+\Gamma_{PSP}$ is below Γ_T. This underestimation of $\Gamma^L_{AN}+\Gamma_{PSP}$ at small distances comes probably from the fact that parallel velocity effects have not been included in the calculation of the PSP transition rate. As the present calculation has been performed with $v_\parallel=0$, below $s_0\simeq1$ a.u. the collective process vanishes due to energy conservation. In the case where the parallel velocity effect would be taken into account ($v_\parallel\neq0$), the collective process would be allowed up to $s=0$ in such a way that the sum $\Gamma^L_{AN}+\Gamma_{PSP}$ would be increased at small distances.

Therefore, the results presented here show that the population of the triplet state $1s2s\ ^3S_1$ by the resonant mode at large distances followed by the IAD mode is not necessary to account for the experimental result, so that the AN and PSP processes play the dominant role in $He^+(1s)$-Al reactions. We believe that the triplet-state population mechanism, which seems to be strongly parallel velocity dependent, is very weak. Further works including parallel velocity effects, in particular for the calculation of RN transition rates, are needed to completely clarify this point. These effects are beyond the scope of the present work.

V. CONCLUSION

In this work, we have reported theoretical studies concerning the neutralization of He^+ ions at Al surfaces under grazing incidence. In a first step, we have calculated the transition rates for the surface-plasmon-assisted mode of ion neutralization at surfaces [which we call the pure surface-plasmon (PSP) process] in the frame of both the orthogonal-

ized first Born approximation and the fixed ion approximation. A comparison between the PSP transition rate and Auger neutralization rates previously calculated by various authors [14–16] shows that the PSP rate dominates for ion-surface distances greater than 1 a.u.; below this distance, the PSP rate vanishes due to energy conservation because parallel velocity effects are not considered in the present calculations.

In a second step, these transition rates are introduced in a set of semiclassical rate equations in order to obtain the neutralized fractions and angular distributions of scattered neutral atoms. Consideration of the PSP process alone leads to an angular distribution pretty close to the experimental distribution obtained in Ref. [17] for 2-keV He^+ ions impinging on an Al(111) surface with 0.5° of incidence. That is not the case when only the AN process is taken into account. However, consideration of both the PSP rates and the AN rates of Refs. [15,16] makes the agreement with the experiment very good at large angles.

Finally, we have implemented a fitting procedure analogous to the one proposed in Ref. [17] in order to extract transition rates from an experimental angular distribution of scattered neutral particles. Instead of introducing the triplet-state $1s2s\ ^3S_1$ population mechanism considered in [17], we have introduced the total rate (which contains all the contributions to the ground state, i.e., AN and PSP contributions) as the sum of two exponential decays depending on adjustable parameters. Our results show that there is no need to introduce the triplet-state population mechanism in order to account for the experimental results and that the AN and PSP processes play the dominant role in low-perpendicular-energy $He^+(1s)$-Al reactions. Furthermore, we believe that any intention to consider the triplet state will necessarily involve inclusion of parallel velocity effects, which are known to affect drastically the resonant transition rates.

ACKNOWLEDGMENTS

The collaboration between the Atomic Collisions group at CELIA (Bordeaux, France) and FAG (Concepción, Chile) has been partially supported by the program ECOS/CONICYT, Grant No. C99E01 and also by the project FONDECYT-1000311 (Chile). The authors wish also to thank the Centre de Ressources Informatique (CRI) de l'Université de Bordeaux-1 where the calculations have been performed.

[1] R. W. Gurney, Phys. Rev. **47**, 479 (1935); J. W. Gadzuk, Surf. Sci. **6**, 133 (1967); **6**, 159 (1967).
[2] S. S. Shekhter, Zh. Eksp. Teor. Fiz. **7**, 750 (1937) [Sov. Phys. JETP **7**, 750 (1937)]; H. D. Hagstrum, Phys. Rev. **96**, 336 (1954); **122**, 83 (1961).
[3] A. A. Almulhem and M. D. Girardeau, Surf. Sci. **210**, 138 (1989); F. A. Gutierrez and J. Díaz-Valdéz, in *Surfaces, Vacuum and their Applications*, edited by Isaac Hernandez-Calderon and Rene Aromoza, AIP Conf. Proc. No. 378 (AIP, Woodbury, NY, 1995), p. 619.
[4] F. A. Gutierrez, Surf. Sci. **370**, 77 (1997).
[5] R. A. Baragiola and C. A. Dukes, Phys. Rev. Lett. **76**, 2547 (1996).
[6] D. Niemann, M. Grether, M. Rösler, and N. Stolterfoht, Phys. Rev. Lett. **80**, 3328 (1998); Nucl. Instrum. Methods Phys. Res. B **146**, 70 (1998).
[7] H. Winter, Nucl. Instrum. Methods Phys. Res. B **78**, 38 (1993).
[8] A. G. Borisov, D. Teillet-Billy, and J. P. Gauyacq, Nucl. Instrum. Methods Phys. Res. B **78**, 49 (1993); F. Martín and M. F. Politis, Surf. Sci. **356**, 247 (1996).
[9] F. A. Gutierrez, S. Jequier, and H. Jouin, Phys. Lett. A **250**, 349 (1998).
[10] G. E. Makhmetov, A. G. Borisov, D. Teillet-Billy, and J. P. Gauyacq, Europhys. Lett. **27**, 247 (1994); G. E. Makhmetov, A. G. Borisov, D. Teillet-Billy, and J. P. Gauyacq, Nucl. Instrum. Methods Phys. Res. B **100**, 342 (1995).
[11] G. E. Makhmetov, A. G. Borisov, D. Teillet-Billy, and J. P. Gauyacq, Surf. Sci. **339**, 182 (1995).
[12] H. Jouin, F. A. Gutierrez, and C. Harel, Surf. Sci. **417**, 18 (1998).
[13] A. Liebsch, *Electronic Excitations at Metal Surfaces* (Plenum, New York, 1997).
[14] M. Alducin, A. Arnau, and P. M. Echenique, Nucl. Instrum. Methods Phys. Res. B **67**, 157 (1992).
[15] N. Lorente and R. Monreal, Surf. Sci. **370**, 324 (1997).
[16] N. Lorente, M. A. Cazalilla, J. P. Gauyacq, D. Teillet-Billy, and P. M. Echenique, Surf. Sci. **411**, L888 (1998); M. A. Cazalilla, N. Lorente, R. Díez-Muiño, J. P. Gauyacq, D. Teillet-Billy, and P. M. Echenique, Phys. Rev. B **58**, 13 991 (1998).
[17] T. Hecht, H. Winter, and A. G. Borisov, Surf. Sci. **406**, L607 (1998).
[18] M. Alducin, Phys. Rev. A **53**, 4222 (1996).
[19] J. Los and J. J. C. Geerlings, Phys. Rep. **190**, 135 (1990); J. Burgdörfer, E. Kupfer, and H. Gabriel, Phys. Rev. A **35**, 4963 (1987); R. Zimny and Z. L. Miskovic, Nucl. Instrum. Methods Phys. Res. B **58**, 387 (1991); B. A. Trubnikov and Yu. N. Yavlinskii, Zh. Eksp. Teor. Fiz. **52**, 1638 (1967) [Sov. Phys. JETP **25**, 1089 (1967)].
[20] N. Lorente and R. Monreal, Phys. Rev. B **53**, 9622 (1996).
[21] C. Denton, J. L. Gervasoni, R. O. Barrachina, and N. R. Arista, Phys. Rev. A **57**, 4498 (1998).
[22] C. J. Powell, Phys. Rev. **175**, 972 (1968).
[23] K. D. Tsuei, E. W. Plummer, A. Liebsch, K. Kempa, and P. Bakshi, Phys. Rev. Lett. **64**, 44 (1990); K. D. Tsuei, E. W. Plummer, A. Liebsch, E. Pehlke, K. Kempa, and P. Bakshi, Surf. Sci. **247**, 302 (1991).
[24] P. J. Jennings, R. O. Jones, and H. Weinert, Phys. Rev. B **37**, 6113 (1988).
[25] H. Jouin, F. A. Gutierrez, C. Harel, S. Jequier, and J. Rangama, Nucl. Instrum. Methods Phys. Res. B **164-165**, 595 (2000).
[26] C. Bottcher, J. Phys. B **6**, 2368 (1973).
[27] F. A. Gutierrez, H. Jouin, S. Jequier, and M. Riquelme, Surf. Sci. **431**, 269 (1999).

[28] H. A. Bethe and E. E. Salpeter, *Quantum Mechanics of One and Two-electron Atoms* (Plenum, New York, 1977).
[29] D. S. Gemmel, Rev. Mod. Phys. **46**, 129 (1974).
[30] J. P. Ziegler, J. P. Biersack, and U. Littmark, *The Stopping and Range of Ions in Solids* (Pergamon, New York, 1985).
[31] P. A. Serena, J. M. Soler, and N. Garcia, Europhys. Lett. **8**, 185 (1989).
[32] M. Kato, R. S. Williams, and M. Aono, Nucl. Instrum. Methods Phys. Res. B **33**, 462 (1988).
[33] H. Winter and J. Leuker, Nucl. Instrum. Methods Phys. Res. B **72**, 1 (1992); H. Winter, Europhys. Lett. **18**, 207 (1992); H. Winter, Phys. Rev. A **46**, R13 (1993).
[34] B. van Someren, P. A. Zeijlmans van Emmichoven, and A. Niehaus, Phys. Rev. A **61**, 022902 (2000).
[35] J. Merino, N. Lorente, W. More, F. Flores, and M. Yu. Gusev, Nucl. Instrum. Methods Phys. Res. B **125**, 250 (1997).
[36] E. C. Goldberg, R. Monreal, F. Flores, H. H. Brongersma, and P. Bauer, Surf. Sci. **440**, L875 (1999).